science, engineering and health studies

Research Article

Science, Engineering and Health Studies
https://lio1.tci-thaijo.org/index.php/sehs
ISSN (Online): 2630-0087

Fabrication of nitrogen and sulfur co-doped carbon dots for antioxidant applications

Koranat Dechsri[1], Supusson Pengnam[1,2], Thapakorn Charoenying[1,2], Nattawat Nattapulwat[1], Tanasait Ngawhirunpat[1], Theerasak Rojanarata[1], and Praneet Opanasopit[1,2]*

[1] Pharmaceutical Development of Green Innovations Group (PDGIG), Faculty of Pharmacy, Silpakorn University, Nakhon Pathom 73000, Thailand
[2] Research and Innovation Center for Advanced Therapy Medicinal Products, Faculty of Pharmacy, Silpakorn University, Nakhon Pathom 73000, Thailand

***Corresponding author**: Praneet Opanasopit
opanasopit_p@su.ac.th

***Received**: 26 March 2025*
***Revised**: 9 July 2025*
***Accepted**: 12 September 2025*
***Published**: 11 November 2025*

***Citation**: Dechsri, K., Pengnam, S., Charoenying, T., Nattapulwat, N., Ngawhirunpat, T., Rojanarata, T., & Opanasopit, P. (2025). Fabrication of nitrogen and sulfur co-doped carbon dots for antioxidant applications. Science, Engineering and Health Studies, 19, 25050007.*

ABSTRACT

Carbon dots (CDs) have attracted attention because of their unique optical properties, biocompatibility, and ease of synthesis. Recently, CDs have demonstrated significant antioxidant activity due to their high surface functionalization, which enables them to effectively interact with reactive oxygen species (ROS) and free radicals. In this study, we aimed to synthesize nitrogen and sulfur co-doped carbon dots (NS-CDs) using a microwave-assisted pyrolysis method, incorporating varying concentrations of nitrogen and sulfur. The particle size, polydispersity index (PDI), zeta potential, and antioxidant activity were evaluated. The optimal formulation, 20-NS-CDs, was further assessed for total phenolic content and intracellular ROS. Finally, biocompatibility was evaluated using an MTT assay. The results revealed that the 20-NS-CDs had a particle size of 4.35 ± 1.84 nm and demonstrated the highest antioxidant activity, as indicated by the lowest half-maximal inhibitory concentration (IC_{50}) value of approximately 0.96 ± 0.03 mg/mL. The total phenolic content was 21.1 ± 1.27 mg of gallic acid equivalent per gram (mg GAE/g), consistent with previous studies, and the antioxidant activity was confirmed by a reduction in intracellular fluorescence in a dose-dependent manner. Therefore, the ability of 20-NS-CDs to scavenge free radicals holds significant potential for applications in health and environmental sciences.

Keywords: antioxidants; carbon dots; nitrogen; reactive oxygen species; sulfur

1. INTRODUCTION

Antioxidants have become increasingly important in modern health and wellness because they protect the body from damage caused by free radicals (Lobo et al., 2010; Zehiroglu & Ozturk Sarikaya, 2019). Free radicals are unstable molecules produced during normal bodily functions, such as metabolism and from external factors such as pollution, UV radiation, and smoking. Free radicals can lead to oxidative stress, resulting in cellular damage, premature aging, and chronic diseases such as heart disease, cancer, and diabetes (Martemucci et al., 2022; Tumilaar et al., 2024). Antioxidants, such as vitamins C and E, beta-carotene, and polyphenols found in fruits, vegetables, and other natural sources neutralize free radicals, helping to prevent or reduce their harmful effects (Kalogerakou & Antoniadou, 2024). Additionally, antioxidants can support the immune system, reduce inflammation, and protect

against age-related conditions, such as wrinkles and cognitive decline. Due to the growing awareness of the importance of prevention and healthy aging, antioxidants have gained popularity in dietary supplements and skincare products. Their potential to promote overall health, reduce disease risk, and slow aging has made them a key component of modern health strategies (Fusco et al., 2007; Sadowska-Bartosz & Bartosz, 2014).

In addition to natural antioxidants, nanoparticles that act as antioxidants have become a fascinating area of research due to their potential to protect cells and tissues from oxidative stress in recent years (Samrot et al., 2022; Sandhir et al., 2015). These nanoparticles, typically made from materials like metals, metal oxides, or organic compounds, exhibit unique properties due to their extremely small size, often in the range of 1-100 nm (Altammar, 2023). This small size allows them to interact with biological systems in novel ways, enhancing their ability to scavenge free radicals and reactive oxygen species (ROS), which are known to contribute to aging and various diseases (Fallah et al., 2024). The antioxidant properties of nanoparticles can be attributed to their high surface area-to-volume ratio, which allows for greater interaction with free radicals. For instance, nanoparticles of zinc oxide, titanium dioxide, gold, and carbon dots have been shown to have significant antioxidant activity. These nanoparticles can be used in various applications, including drug delivery systems, food preservation, and cosmetics, offering a new way to enhance the effectiveness of antioxidants in treating or preventing oxidative stress-related conditions (Abbasi et al., 2023; Karnwal et al., 2024; Samrot et al., 2022).

Carbon dots (CDs), a class of zero-dimensional carbon nanoparticles, have attracted significant attention recently due to their unique optical properties, biocompatibility, and ease of surface functionalization (Liu et al., 2020; Qureshi et al., 2024). These properties make them promising candidates for various applications, including bioimaging, drug delivery, sensors, and environmental remediation (Cui et al., 2021; Magesh et al., 2022). The use of CDs has especially increased in biomedical applications, including anticancer, antibacterial, and antifungal therapies. One of the most promising applications of CDs is their antioxidant activity (C.-Y. Wang et al., 2023; D. Wang et al., 2025). Their ability to scavenge free radicals and reactive oxygen species prevents oxidative stress and related diseases (Gedda et al., 2023). When synthesizing carbon dots for antioxidant purposes, selecting suitable carbon sources is critical to ensure high-quality CDs with enhanced biological activity. Common precursors include natural organic materials like fruit and vegetable extracts (e.g., citrus, apples, bananas, and spinach), which are rich in polyphenols and antioxidants (Brglez Mojzer et al., 2016). Plant-based biomass, such as lignin, cellulose, and chitosan (derived from shells), is frequently used to create CDs with improved biocompatibility and antioxidant properties (Waseem Basha et al., 2024). CDs can function as antioxidants through two main mechanisms: improving electron donation and increasing the availability of active sites (Gulcin, 2020; Kasif et al., 2024).

Improving the electron donation ability of carbon dots is crucial for their effectiveness as antioxidants. Electron donation refers to the ability of materials to donate electrons during chemical reactions, particularly in antioxidant activity. Free radicals and ROS are highly reactive due to their unpaired electrons, and antioxidants neutralize them by donating electrons, stabilizing these harmful molecules, and preventing cellular damage. The electron donation capacity of CDs can be enhanced by modifying their surface by introducing functional groups (such as hydroxyl or amino groups) or doping with elements like nitrogen (N) or sulfur (S). These adjustments strengthen the capacity of CDs to interact with and neutralize free radicals (Ji et al., 2019; Kasif et al., 2024; Ngoc et al., 2023).

Increasing the availability of active sites for free radical scavenging is another key strategy to enhance the antioxidant potential of carbon dots. Active sites are specific regions on the surface of carbon dots where interactions with free radicals or ROS occur. The more active sites that are available, the more effective the CDs will be at neutralizing free radicals. Increasing the availability of these sites can be achieved by modifying the surface area of CDs, either by making them smaller and porous or by incorporating functional groups that increase reactivity. Additionally, doping the CDs with specific elements can improve the available reactive sites. This method allows the CDs to interact with multiple free radicals simultaneously, improving their overall antioxidant activity (Innocenzi & Stagi, 2023; Kasif et al., 2024; Zhang et al., 2018).

The antioxidant properties of carbon dots are also influenced by size, surface chemistry, and doping with heteroatoms like nitrogen and sulfur. Recent studies have shown that incorporating N and S into the CD structure enhances their antioxidant activity, likely by improving their electron donation ability and increasing the availability of active sites. Co-doping with nitrogen and sulfur can offer synergistic effects, optimizing the antioxidant properties of these nanomaterials (Kasif et al., 2024; Zhang et al., 2018).

In recent years, green synthesis has gained significant attention as an environmentally friendly and sustainable approach to fabricating nanomaterials, offering advantages such as reduced toxicity, cost-effectiveness, and minimal environmental impact (Afonso et al., 2024; Ahmed et al., 2022). Citric acid (CA), a naturally occurring organic acid found in citrus fruits, is widely recognized for its safety, biodegradability, and diverse applications in food, medicine, and cleaning products. Due to its low toxicity and classification as generally recognized as safe (GRAS) by regulatory authorities, citric acid is an excellent precursor for synthesizing carbon dots (Johny et al., 2024; Ren et al., 2021). In addition, microwave-assisted synthesis has gained attention as a green and efficient technique for producing carbon dots and other nanomaterials (Romero et al., 2021; Yalshetti et al., 2024). Compared to conventional heating methods, microwave digestion provides rapid, uniform, and direct energy transfer, significantly reducing reaction times and energy consumption (Lozano Pérez et al., 2024). This method often allows for using water as a solvent, eliminating the need for hazardous chemicals and minimizing environmental impact (Kumar et al., 2020). Additionally, microwave-assisted synthesis typically operates at lower temperatures, ensuring high product yield while maintaining eco-friendly processing conditions (Thanayutsiri et al., 2020).

Many studies have reported the synthesis of CDs using citric acid and L-cysteine (CYS) as carbon and heteroatom sources. One standard method is using a microwave oven,

which is fast and straightforward. However, this method lacks precise control over the reaction conditions. In addition, previous studies often used only one fixed ratio of citric acid to L-cysteine, without exploring how different amounts of nitrogen and sulfur affect the properties of the CDs, especially their antioxidant activity (Suner et al., 2021).

In this study, we used a microwave pyrolysis method that enabled better control of the reaction process. We also varied the ratio of citric acid and L-cysteine to investigate how increased nitrogen and sulfur content influences the antioxidant activity of the CDs. This approach provides a clearer understanding of the relationship between doping level and antioxidant performance, which may help in designing CDs for biomedical and environmental applications.

In this study, we aim to fabricate nitrogen- and sulfur-codoped carbon dots (NS-CDs) with enhanced antioxidant properties using citric acid as a carbon source through the microwave digestion technique. We carefully controlled the doping process and explored various nitrogen and sulfur ratios. We sought to identify the optimal conditions for maximizing the antioxidant activity of the carbon dots. The resulting NS-CDs will be characterized for their structural, optical, and antioxidant properties to evaluate their effectiveness in combating oxidative stress.

2. MATERIALS AND METHODS

The chemical reagents used in the study were citric acid monohydrate and L-cysteine, which were obtained from Merck KGaA (Darmstadt, Germany). 2,2-diphenyl-1-picrylhydrazyl (DPPH), 3-(4,5-Dimethyl-2-thiazolyl)-2,5-diphenyl-2H-tetrazolium bromide (MTT), ascorbic acid, Folin-Ciocalteu's phenol (F-C) reagent, gallic acid monohydrate, and sodium carbonate were purchased from Sigma-Aldrich (St. Louis, MO, USA). The cell-permeant 2',7'-dichlorodihydrofluorescein diacetate (H_2DCFDA) was obtained from Invitrogen (Carlsbad, CA, USA). Normal human fibroblast (NHF) cell lines, used as a model for normal cells to evaluate biocompatibility, were obtained from the American Type Culture Collection (ATCC, Rockville, MD, USA). Cell culture reagents, including fetal bovine serum (FBS), penicillin-streptomycin, trypsin-EDTA, and Dulbecco's Modified Eagle's Medium (DMEM), were obtained from Gibco BRL (Rockville, MD, USA). Ultrapure water was prepared using a Milli-Q system (Millipore, USA). All other chemicals and solvents were used as received without further purification.

2.1 Fabrication of NS-CDs

NS-CDs synthesized using various mole ratios of carbon sources to heteroatoms, including nitrogen and sulfur. Citric acid and L-cysteine were used as the carbon source and heteroatom precursors. The C/N-S ratios were varied as 1:0.01, 1:0.025, 1:0.05, 1:0.10, and 1:0.20 to obtain 1-NS-CDs, 2.5-NS-CDs, 5-NS-CDs, 10-NS-CDs, and 20-NS-CDs, respectively. For a typical synthesis of N, S-CDs with a 1:0.01 ratio, 0.03 moles of citric acid and 0.0003 moles of L-cysteine were dissolved in 20 mL of distilled water and mixed slowly at room temperature to form a homogeneous solution. This mixture was then transferred to a 35-mL reaction vessel, and the solution was subjected to microwave synthesis at 180°C for 10 min using a CEM Discover SP microwave instrument (CEM Corporation, Matthews, NC, USA). After the reaction, the NS-CDs dispersion was centrifuged at 12,000 rpm for 10 min to remove large particles. The resulting dispersion was dialyzed in a centrifuge tube filter (MWCO = 3 kDa) at 5,000 rpm for 15 min to eliminate excess precursors. Finally, the purified supernatant was stored in a refrigerator at 4°C for future use.

2.2 Characterization of NS-CDs

The particle size, polydispersity index (PDI), and zeta potential of the NS-CDs dispersion were measured using a dynamic light scattering (DLS) particle size analyzer (Zetasizer Nano-ZS, Malvern Instruments, Worcestershire, UK), with data collected in triplicate. Before measurement, the dispersion was diluted with deionized water at a ratio of 1:99 (NS-CDs dispersion to deionized water). UV-Vis absorption spectra of 20-NS-CDs were recorded and compared with pure citric acid and L-cysteine using a UV-Vis scanning spectrophotometer (Cary 60 UV-Vis, Agilent Technologies, USA) over the range of 200–800 nm. Furthermore, the fluorescence of 20-NS-CDs was observed under a UV lamp at 365 nm. Attenuated total reflectance Fourier-transform infrared (ATR-FTIR) spectroscopy (Nicolet iS5, Thermo Fisher Scientific, MA, USA) was performed at a resolution of 4 cm^{-1} with 16 scans, covering a range from 500 to 4000 cm^{-1} to acquire the spectra of all formulations of NS-CDs spectra. X-ray diffraction (XRD) pattern of 20-NS-CDs was captured using an X-ray diffractometer (Malvern Panalytical, Aeris Benchtop XRD System) at a 2°/min scanning rate within a 10–50° range. The excitation-dependent emission spectrum of the 20-NS-CDs dispersion was analyzed using a spectrofluorophotometer (RF-6000, Bara Scientific Co., Ltd., Shimadzu, Japan) with excitation wavelengths ranging from 300 to 400 nm. In addition, the % yield of all formulations was also calculated.

2.3 Assessment of antioxidant activity

The antioxidant activity was assessed using the DPPH free radical scavenging assay, which was modified based on a previous study (Dechsri et al., 2024c). All formulations were prepared in distilled water at various concentrations (50, 125, 250, 500, 1250, 2500, and 5000 µg/mL). Each concentration of NS-CDs dispersion was then mixed with a freshly prepared DPPH ethanolic solution at a 1:1 volume ratio, resulting in a final DPPH concentration of approximately 0.004%. The mixture was incubated in the dark at room temperature for 30 min to allow the scavenging reaction. After incubation, the absorbance of the solution was measured at 520 nm using a multimode microplate reader (VICTOR Nivo™ Multimode Plate Reader, PerkinElmer, Germany). Vitamin C and a DPPH solution without NS-CDs dispersion were used as positive and negative controls, respectively. The inhibition of DPPH radicals was calculated as a percentage using Equation (1). Additionally, the IC_{50} values (half-maximal inhibitory concentration) of the NS-CDs dispersion were determined through linear regression analysis.

$$Inhibition\ (\%) = \frac{Abs.\ of\ control\ -\ Abs.\ of\ sample}{Abs.\ of\ control} \times 100 \quad (1)$$

Where Abs. of control is the absorbance of the DPPH solution without the NS-CDs dispersion. Abs. of sample is the absorbance of the DPPH solution with the NS-CDs dispersion.

2.4 Determination of total phenolic content

The total phenolic content (TPC) of 20-NS-CDs was investigated using the Folin-Ciocalteu method by adjusting the previous protocol (Molole et al., 2022). The reaction mixtures were prepared according to the previously outlined procedure. Gallic acid (GA) calibration solutions with concentrations of 10, 20, 40, 60, 80, and 100 µg/mL were prepared in triplicate. The Folin-Ciocalteu's phenol reagent was freshly prepared with distilled water in a 1:10 ratio. A sodium carbonate (Na_2CO_3) solution (7.5% w/v) was also prepared using distilled water. The dispersion of 20-NS-CDs was prepared in distilled water at 1000 µg/mL. Briefly, 20 µL of the sample and 20 µL of 10% (v/v) F-C was added into a test tube and mixed thoroughly using a vortex mixer for 2 min. Subsequently, 160 µL of 7.5% (w/v) Na_2CO_3 solution was pipetted into the tube and mixed well with the vortex mixer. The test tube was then placed in the dark at room temperature for 30 min, and the absorbance was measured at 700 nm. All measurements were performed in triplicate. The total phenolic content was determined using the calibration curve from gallic acid, and the results were reported as mg of gallic acid equivalent per gram (mg GAE/g) of the 20-NS-CDs, using the following Equation (2).

$$C\ (mg\ GAE/g) = C_1(mg/mL) \times \frac{V\ (mL)}{M\ (g)} \quad (2)$$

Where C is the total phenolic compound in mg of gallic acid equivalent per gram (mg GAE/g)
C_1 is the concentration of gallic acid in the 20-N S-CDs, which was estimated from the gallic acid calibration curve (mg/mL).
V is the volume of the 20-NS-CDs (mL)
M is the weight of the 20-NS-CDs (g)

2.5 Evaluation of antioxidant effect: determination of intracellular ROS

The dichlorofluorescein diacetate (DCFDA) assay was used to assess the ability of 20-NS-CDs to reduce intracellular reactive oxygen species. Normal human fibroblast cells were seeded in a 96-well plate at a density of 25,000 cells per well and incubated for 24 hours at 37°C with 5% CO_2. After the incubation, the medium was removed, and 0.1 mM H_2O_2 was added to induce ROS (positive control) for 1 hour. Following ROS induction, fresh media containing different concentrations of 20-NS-CDs (50 µg/mL, 500 µg/mL, and 5000 µg/mL) were added, and the cells were incubated for an additional 24 hours under the same conditions. After this, the medium was replaced with 100 µL of H_2DCFDA (prepared in reduced serum to a final concentration of 20 µM) and incubated for 30 min in the dark. The cells were washed twice with phosphate-buffered saline (PBS) and then replaced with 100 µL of PBS. Fluorescence intensity was measured using a microplate reader at excitation and emission wavelengths of 485 nm and 535 nm, respectively. The percentage of intracellular ROS was calculated using equation (3). In addition, untreated cells were applied as a control group.

$$Intracellular\ ROS\ (\%) = \frac{Fluorescence\ (sample)}{Fluorescence\ (control)} \times 100\% \quad (3)$$

Furthermore, the percentage of ROS inhibition compared to the H_2O_2 group can be calculated using equation (4).

$$ROS\ Inhibition\ (\%) = \frac{Fluorescence\ (H_2O_2) - Fluorescence\ (sample)}{Fluorescence\ (H_2O_2) - Fluorescence\ (control)} \times 100 \quad (4)$$

2.6 Biocompatibility assessment

NHF cell lines were maintained in controlled incubators at 37°C with 5% CO_2, using a DMEM culture medium supplemented with 10% FBS and 1% penicillin-streptomycin. Cell growth was monitored under an inverted microscope (Nikon® T-DH, Nikon, Tokyo, Japan) until the cells reached 70–80% confluency. Once this was achieved, the cells were subcultured and seeded into 96-well plates at a density of 1×10^4 cells per well for the MTT assay experiment. The MTT assay was conducted following ISO 10993-5: 2009 guidelines. Briefly, after the cells were fully seeded, the plate was incubated for 24 hours. The culture medium was then replaced with the 20-NS-CDs dispersion at various concentrations (0.01–20 mg/mL) and incubated for 24 hours. To assess cell viability, 25 µL of MTT solution (5 mg/mL) was added to each well and incubated for 3 hours at 37°C, allowing for the formation of formazan crystals in viable cells. After incubation, the medium was replaced with 100 µL of dimethyl sulfoxide (DMSO) to dissolve the formed crystals, resulting in a bluish-violet solution. The absorbance at 550 nm was then measured using a microplate reader to evaluate cell viability. Cell viability was calculated using Equation (5). Untreated cells served as the control group.

$$Cell\ viability\ (\%) = \frac{Abs.\ of\ sample}{Abs.\ of\ control} \times 100\% \quad (5)$$

Where Abs. of control is the absorbance of the cells without the NS-CDs dispersion. Abs. of sample is the absorbance of the cells with the NS-CDs dispersion.

2.7 Statistical analysis

The experiments were conducted in triplicate, and the results are presented as the mean ± standard deviation (S.D.). Statistical analyses were carried out using the independent t-test and F-test in IBM SPSS Statistics version 28, with a 95% confidence level. Differences were considered statistically significant at a p-value of less than 0.05.

3. RESULTS AND DISCUSSION

3.1 Preparation of NS-CDs

The NS-CDs dispersion was prepared by combining citric acid and L-cysteine using a microwave synthesis technique. After a 10-minute reaction time, the solution turned into a yellow dispersion. The particle size, polydispersity index, and zeta potential were measured using a dynamic light scattering particle size analyzer. The results, presented in Table 1, indicate that the concentration of nitrogen and sulfur dopants significantly influences the particle size and zeta potential of the carbon dots. As the concentration of nitrogen and sulfur dopants in the synthesis of carbon dots increases, the particle size tends to increase, as seen in the previous reports (Ding et al., 2014; Zhou et al., 2022). For instance, 1-NS-CDs (with low doping concentration) exhibit a relatively small particle size of 1.60 ± 0.22 nm. As the dopant concentration increases, the particle size grows, with 2.5-NS-CDs and 5-NS-CDs having particle sizes of 1.79 ± 0.26 nm and 1.83 ± 0.20 nm, respectively. At even higher doping concentrations,

such as 10-NS-CDs, and 20-NS-CDs, the particle size increases further, with 20-NS-CDs showing the largest particle size of 4.35 ± 1.84 nm. Nitrogen and sulfur atoms can influence the nucleation and growth processes of the carbon dots during synthesis. Higher dopant concentrations may act as sites for particle growth, leading to larger sizes (Hu et al., 2014; Shahid et al., 2023). For example, nitrogen doping may enhance the stability of the carbon core, reducing aggregation while allowing the carbon dots to grow larger (Ozyurt et al., 2023). Similarly, sulfur doping may influence the formation of the carbon network and interparticle interactions, promoting particle growth. The PDI values of all formulations are still below 0.5, which is generally considered acceptable for a relatively narrow distribution (Gao et al., 2020; Moammeri et al., 2023). In addition, the zeta potential was observed to increase. This could be attributed to nitrogen and sulfur groups on the surface of the NS-CDs derived from the citric acid and cysteine powder used as precursors. Incorporating these functional groups likely enhances the surface charge, increasing zeta potential (Lu et al., 2019; Zhang et al., 2022). However, the zeta potential of all formulations is close to neutral. They can still theoretically function as antioxidants. This is because antioxidant activity is more strongly influenced by factors such as surface functional groups, chemical structure, and heteroatom doping (e.g., nitrogen and sulfur) than by surface charge alone (Zhang et al., 2018). In addition, the % yield of all formulations was also reported in Table 1. All formulations achieved a percentage yield ranging from 56% to 60%, consistent with previous research findings (Huang & Ren, 2025).

Table 1. Particle size, PDI, zeta potential, and percentage of yield of all formulations

Formulations	Particle size (nm)	PDI	Zeta potential (mV)	Yield (%)
1-NS-CDs	1.60 ± 0.22	0.17 ± 0.08	-0.42 ± 2.18	60.44 ± 1.65
2.5-NS-CDs	1.79 ± 0.26	0.09 ± 0.03	0.32 ± 1.48	57.96 ± 0.85
5-NS-CDs	1.83 ± 0.20	0.24 ± 0.01	0.52 ± 0.93	59.86 ± 0.94
10-NS-CDs	2.31 ± 0.19	0.22 ± 0.06	0.89 ± 0.83	56.15 ± 1.13
20-NS-CDs	4.35 ± 1.84	0.31 ± 0.05	1.09 ± 0.45	55.77 ± 0.96

3.2 Characterization of NS-CDs

As illustrated in Figure 1a, the UV-visible absorption spectrum of 20-NS-CDs (orange line) peaked at 365 nm, extending to 700 nm. The absorption at 365 nm is associated with the n−π* transition of C═O/C═N bonds, aligning with previous studies (Dechsri et al., 2024a; Liu, 2020). In contrast, the citric acid and L-cysteine solutions, represented by the green and blue lines, respectively, which served as precursors, displayed no detectable peaks (Huang et al., 2019). The difference in UV-Vis spectra between the precursor solutions and 20-NS-CDs suggests the successful completion of the carbon dots synthesis. These findings are consistent with prior reports (Ehtesabi & Massah, 2021). In addition, as shown in the subset of Figure 1a, synthesized 20-NS-CDs exhibited excellent dispersion, appearing as a yellowish transparent solution in natural light and emitting a blue luminescence under UV light at 365 nm (Ding et al., 2014).

As presented in Figure 1b, the 20-NS-CDs displayed fluorescence spectra, with excitation wavelengths ranging from 300 to 400 nm. The photoluminescence spectra of 20-NS-CDs showed the strongest blue fluorescence emission centered at approximately 460 nm when excited at 320 nm, with no noticeable variation under different excitation wavelengths. This suggests that the fluorescence emission wavelength of the 20-NS-CDs is independent of the excitation wavelength, which aligns with previous studies on carbon dots (Kasif et al., 2024; Zhang & He, 2015).

The ATR-FTIR spectra of 20-NS-CDs compared with precursors, including citric acid and L-cysteine, are presented in Figure 1c, highlighting various peaks corresponding to functional groups on their surface. The bands at 3490 cm^{-1} can be attributed to the stretching vibrations of O-H and N-H, while 3290 cm^{-1} can be assigned to the bending vibrations of C-N groups. A broad absorption band around 2880 cm^{-1} signifies the aromatic C-H stretching, while an S-H stretching peak can be observed at 2555 cm^{-1}. The band at 1680 cm^{-1} corresponds to the vibrations of C-O-C bonds, while the peak at 1430 cm^{-1} is attributed to aromatic C=C stretching, which is likely linked to the framework of polycyclic aromatic hydrocarbons in carbon dots. In addition, the fingerprint region at 1335 cm^{-1} corresponding to C-N stretching signifies the presence of an aromatic amine, while the stretching shoulders of C–S appear at 1160 cm^{-1}. Finally, the band at 1078 cm^{-1} corresponds to a distinct C-O-C stretching peak. Therefore, the carbon dot spectral analysis validated the anticipated structure of the synthesized 20-NS-CDs (Dechsri et al., 2024b; Hasan et al., 2018; Suner et al., 2021; Zhang & He, 2015).

As shown in Figure 1d, the XRD pattern of 20-NS-CDs compared with that of citric acid, and L-cysteine. The XRD patterns of citric acid (green line) and L-cysteine (blue line) exhibited sharp peaks at various 2θ values, confirming their crystalline structures as small organic molecules (Umar et al., 2022). Following the synthesis, the XRD pattern of 20-NS-CDs (orange line) revealed multiple intense peaks, with a signal-to-noise ratio exceeding three for several peaks, indicating a polycrystalline structure. A broad diffraction peak centered around 2θ = 22° suggests the presence of an amorphous carbon core characteristic of carbon dots (Pal et al., 2020). Additionally, a strong diffraction peak at a 2θ value of 30.20°, which corresponds to the (002) crystal planes characteristic of graphite composed of sp^2-hybridized carbon atoms, is comparable to other forms of carbon (Kasif et al., 2024; Sharma et al., 2022). Numerous narrow peaks in the XRD pattern highlight the distinct crystallinity of 20-NS-CDs, contrasting with the more amorphous nature observed in other samples. Therefore, the XRD analysis confirms the successful formation of 20-NS-CDs with both crystalline and amorphous characteristics, indicative of their complex structural composition.

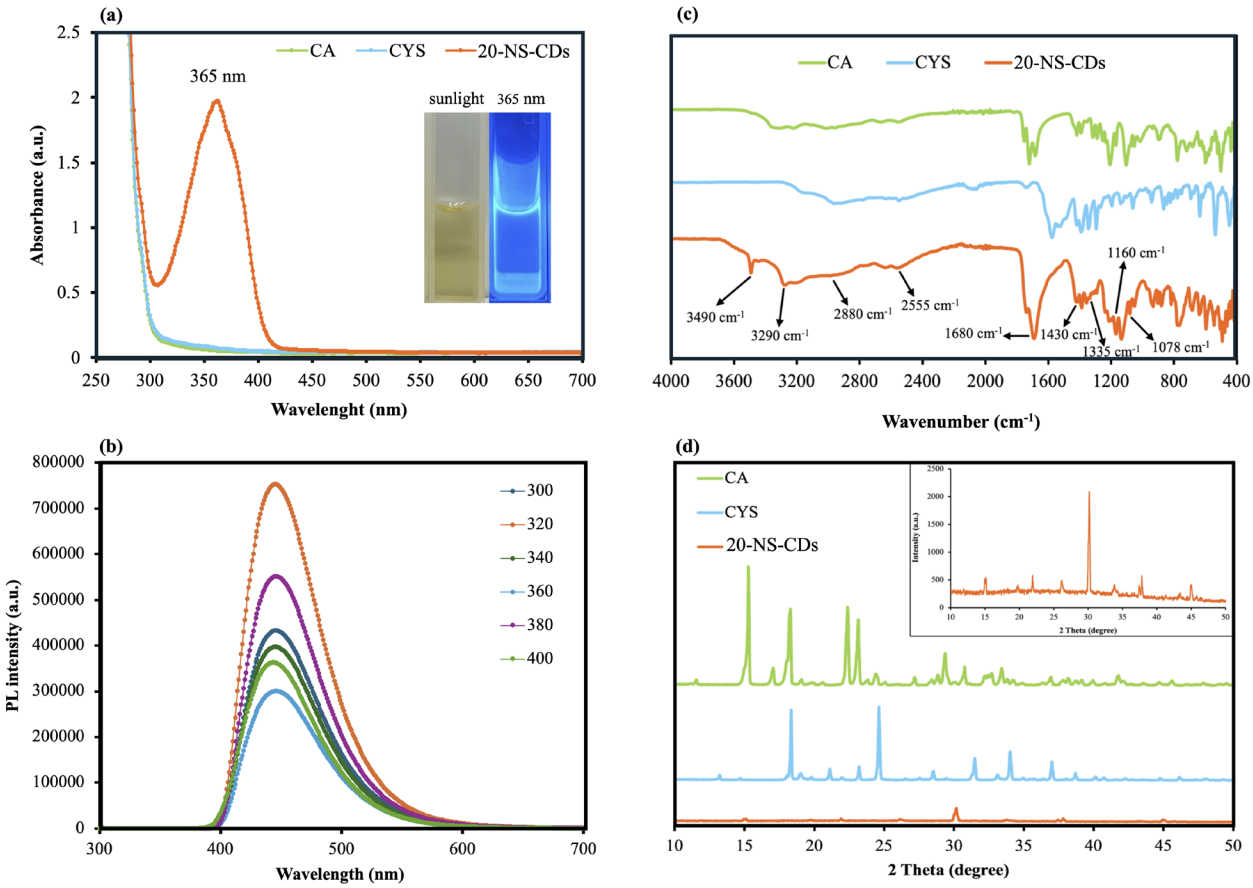

Figure 1. Characterizations of 20-NS-CDs (a) UV-visible spectra and inset with photographs under sunlight (yellow color) and UV lamp 365 nm (blue color), (b) Fluorescence emission spectrum-dependent excitation wavelengths, (c) ATR-FTIR spectra, (d) XRD pattern

3.3 Assessment of antioxidant activity

The DPPH assay is a widely recognized method for assessing the antioxidant activity of nanoparticles, particularly their ability to scavenge free radicals. In this study, NS CDs were synthesized with varying nitrogen and sulfur ratios, and their antioxidant properties were evaluated. A key parameter in the DPPH assay is the IC_{50} value, which represents the concentration required to inhibit 50% of DPPH radicals. A lower IC_{50} value indicates higher antioxidant activity, reflecting a greater ability to neutralize free radicals at lower concentrations. As shown in Table 2, the presence of nitrogen and sulfur functional groups enhances the electron-donating ability, thereby improving radical scavenging (Kasif et al., 2024). Among the tested formulations, 20-NS-CDs exhibited the highest antioxidant activity, as reflected by their lowest IC_{50} value. The high concentration of functional groups in NS-CDs enhances electron transfer, facilitating the effective neutralization of free radicals (Li et al., 2015). Furthermore, doping elements such as sulfur increase the availability of active sites, which play a crucial role in boosting radical scavenging efficiency. This can be further optimized by modifying the surface area, incorporating reactive functional groups, or adjusting the doping ratio, ultimately enhancing the overall antioxidant potential of carbon dots. Therefore, 20-NS-CDs with the lowest IC_{50} value, are more effective antioxidants and could be used in pharmaceutical, food preservation, and biomedical applications where oxidative stress needs to be mitigated.

Table 2. IC_{50} values of antioxidant activity of all formulations

Samples	IC_{50} (mg/mL)
1-NS-CDs	> 5*
2.5-NS-CDs	3.50 ± 0.02*
5-NS-CDs	3.47 ± 0.07*
10-NS-CDs	1.65 ± 0.01*
20-NS-CDs	0.96 ± 0.03

*Significant difference compared to the 20-NS-CDs ($p < 0.05$)

3.4 Determination of total phenolic content

The total phenolic content of 20-NS-CDs was measured using the Folin-Ciocalteu method, with the standard curve derived from gallic acid. The equation of the standard curve is y = 0.0009x - 0.0006, with an R^2 value of 0.9963, as shown in Figure 2. The phenolic composition was found to be 21.1 ± 1.27 mg GAE/g of 20-NS-CDs, which is in close agreement with previous research (Molole et al., 2022). The total phenolic content often correlates with hydroxyl (–OH) groups, particularly in 20-NS-CDs, which is confirmed by ATR-FTIR analyses (Lin et al., 2019). The synthesis of 20-NS-CDs using citric acid, which contains both carboxyl and hydroxyl groups, suggests that phenolic-like structures might form during the condensation reactions that occur during carbon dot formation. These reactions can lead to the creation of these groups on the surface of the

carbon dots. Therefore, the presence of these groups, particularly hydroxyl and carboxyl, can significantly improve the antioxidant properties of the resulting carbon dots (Chen et al., 2020; Ibrayev et al., 2022; Lin et al., 2019).

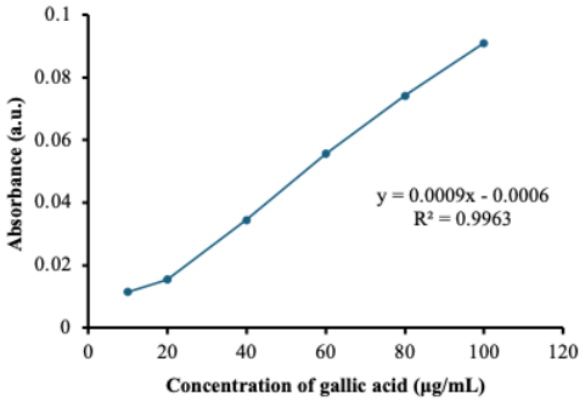

Figure 2. Standard curve of gallic acid at various concentrations for the determination of TPC

3.5 Evaluation of antioxidant effect: determination of intracellular ROS

The ROS levels within NHF cells were assessed using the detection probe DCFH-DA. DCFH-DA is a non-fluorescent molecule that reacts with several ROS, including $^1O_2$ and •OH, to produce fluorescent DCF. In this experiment, untreated NHF cells served as the control group, and H_2O_2 was used to induce ROS to assess the antioxidant effect by measuring the intensity of green fluorescence. As presented in Figure 3, the fluorescent intensity was significant higher in the H_2O_2-treated group compared to the control group, as a result of H_2O_2 being catalyzed to produce free radicals. Moreover, NHF cells treated with increasing concentrations of 20-NS-CDs ranging from 50 to 5000 µg/mL showed reduced intracellular fluorescence of DCF in a dose-dependent manner. These findings suggest that 20-NS-CDs could be used as an antioxidant, which is consistent with the previously mentioned DPPH results (Swain & Jena, 2025).

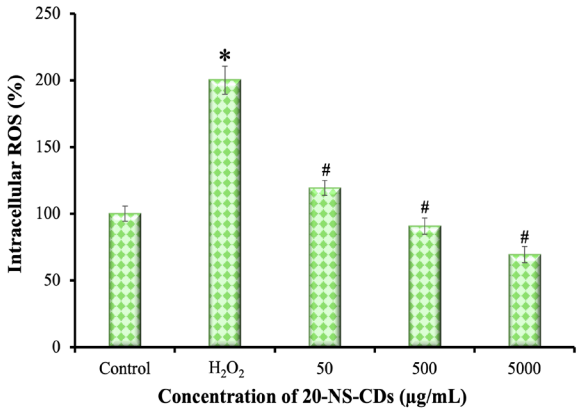

Figure 3. Intracellular ROS levels were determined using a DCFH-DA ROS probe in HNF cell lines. *p<0.05 and $^{\#}p$<0.05 compared with control and H_2O_2, respectively

Furthermore, the percentage of ROS inhibition compared to the H_2O_2 group is presented in Table 3. At concentrations of 50, 500, and 5000 µg/mL, the samples showed 74%, 112%, and 141% inhibition of intracellular ROS production, respectively, compared to the H_2O_2-treated group. This trend demonstrates that ROS inhibition increases with sample concentration, consistent with the reduced fluorescence intensity shown in Figure 3.

Table 3. Percentage of ROS inhibition compared to the H_2O_2 group

Concentration of 20-NS-CDs (µg/mL)	% ROS inhibition compared to H_2O_2 group
50	73.76 ± 7.50
500	112.44 ± 8.14
5000	141.38 ± 8.19

3.6 Biocompatibility assessment

The cell viability of NHF cells, used as a model for normal cells, was evaluated after 24 h of exposure to 20-NS-CDs through an MTT assay, as shown in Figure 4. The results demonstrate that the 20-NS-CDs were non-toxic to NHF cells, with all concentrations ranging from 0.01 to 5 mg/mL maintaining cell viability above 70%, following the ISO 10993-5:2009 standards. Furthermore, the control (untreated) cells showed 100% viability. The observed outcomes may be attributed to the small nanosize and spherical shape of the 20-NS-CDs, which likely contribute to their non-toxic behavior at lower concentrations. These results suggest that 20-NS-CDs possess excellent biocompatibility and non-toxicity, making them promising candidates for biomedical applications such as antioxidant activity (Tian et al., 2020; Tungare et al., 2020).

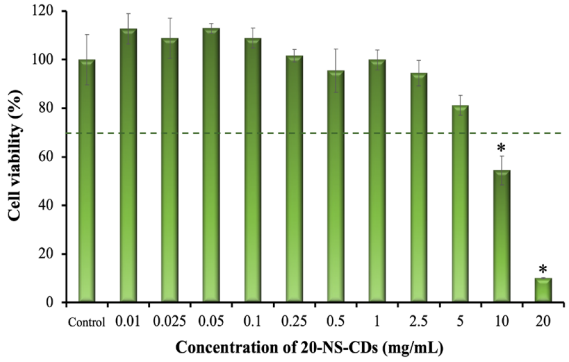

Figure 4. Cell viability of treatment after 24 h with 20-NS-CDs at various concentrations *p<0.05 compared with the control group

4. CONCLUSION

In conclusion, 20-NS-CDs were successfully synthesized using microwave-assisted pyrolysis. These 20-NS-CDs demonstrated biocompatibility with NHF cell lines at concentrations up to 5 mg/mL, and a yield of 55.77%. Regarding antioxidant activity, 20-NS-CDs showed superior performance compared to other formulations, likely due to the high concentration of functional groups in the NS-CDs, which enhance electron transfer and effectively neutralize free radicals. Additionally, the total

phenolic content of 20-NS-CDs was 21.1 ± 1.27 mg GAE/g, which correlates with the presence of hydroxyl groups. In addition, the antioxidant activity was confirmed by a reduction in intracellular fluorescence of DCF in a dose-dependent manner, at concentration ranging from 50 to 5000 µg/mL. These results indicate that 20-NS-CDs are promising nanomedicine with enhanced antioxidant activity, offering potential for applications in the food, pharmaceutical, and environmental industries.

CONFLICT OF INTEREST

There is no conflict of interest to declare.

ACKNOWLEDGMENTS

This research is financially supported by Thailand Science Research and Innovation (TSRI) and the National Science, Research, and Innovation Fund (NSRF) (Fiscal Year 2025). The authors would like to thank Anthony Arthit Phonpituck for English proofreading of the research article.

REFERENCES

Abbasi, R., Shineh, G., Mobaraki, M., Doughty, S., & Tayebi, L. (2023). Structural parameters of nanoparticles affecting their toxicity for biomedical applications: A review. *Journal of Nanoparticle Research*, *25*(3), Article 43. https://doi.org/10.1007/s11051-023-05690-w

Afonso, I. S., Cardoso, B., Nobrega, G., Minas, G., Ribeiro, J. E., & Lima, R. A. (2024). Green synthesis of nanoparticles from olive oil waste for environmental and health applications: A review. *Journal of Environmental Chemical Engineering*, *12*(5), Article 114022. https://doi.org/10.1016/j.jece.2024.114022

Ahmed, S. F., Mofijur, M., Rafa, N., Chowdhury, A. T., Chowdhury, S., Nahrin, M., Islam, A. B. M. S., & Ong, H. C. (2022). Green approaches in synthesising nanomaterials for environmental nanobioremediation: Technological advancements, applications, benefits and challenges. *Environmental Research*, *204*, Article 111967. https://doi.org/10.1016/j.envres.2021.111967

Altammar, K. A. (2023). A review on nanoparticles: Characteristics, synthesis, applications, and challenges. *Frontiers in Microbiology*, *14*, Article 1155622. https://doi.org/10.3389/fmicb.2023.1155622

Brglez Mojzer, E., Knez Hrnčič, M., Škerget, M., Knez, Ž., & Bren, U. (2016). Polyphenols: Extraction methods, antioxidative action, bioavailability and anticarcinogenic effects. *Molecules*, *21*(7), Article 901. https://doi.org/10.3390/molecules21070901

Chen, Y., Qin, X., Yuan, C., & Wang, Y. (2020). Switch on fluorescence mode for determination of L-cysteine with carbon quantum dots and Au nanoparticles as a probe. *RSC Advances*, *10*(4), 1989–1994. https://doi.org/10.1039/C9RA09019C

Cui, L., Ren, X., Sun, M., Liu, H., & Xia, L. (2021). Carbon dots: Synthesis, properties and applications. *Nanomaterials*, *11*(12), Article 3419. https://doi.org/10.3390/nano11123419

Dechsri, K., Suwanchawalit, C., Apirakaramwong, A., Patrojanasophon, P., Rojanarata, T., Opanasopit, P., Pengnam, S., & Charoenying, T. (2024a). Photo-sensitive antibacterial activity of *o*-phenylenediamine carbon dots. *Journal of Current Science and Technology*, *14*(2), Article 36. https://doi.org/10.59796/jcst.V14N2.2024.36

Dechsri, K., Suwanchawalit, C., Patrojanasophon, P., Opanasopit, P., Pengnam, S., Charoenying, T., & Taesotikul, T. (2024b). Photodynamic antibacterial therapy of gallic acid-derived carbon-based nanoparticles (GACNPs): Synthesis, characterization, and hydrogel formulation. *Pharmaceutics*, *16*(2), Article 254. https://doi.org/10.3390/pharmaceutics16020254

Dechsri, K., Suwanchawalit, C., Pengnam, S., Pornpitchanarong, C., Opanasopit, P., & Apirakaramwong, A. (2024c). Antioxidant activity of gallic acid carbon-based nanomaterials. *Science, Engineering and Health Studies*, *18*, Article 24050019. https://doi.org/10.69598/sehs.18.24050019

Ding, H., Wei, J.-S., & Xiong, H.-M. (2014). Nitrogen and sulfur co-doped carbon dots with strong blue luminescence. *Nanoscale*, *6*(22), 13817–13823. https://doi.org/10.1039/C4NR04267K

Ehtesabi, H., & Massah, F. (2021). Improvement of hydrophilicity and cell attachment of polycaprolactone scaffolds using green synthesized carbon dots. *Materials Today Sustainability*, *13*, Article 100075. https://doi.org/10.1016/j.mtsust.2021.100075

Fallah, S., Yusefi-Tanha, E., & Peralta-Videa, J. R. (2024). Interaction of nanoparticles and reactive oxygen species and their impact on macromolecules and plant production. *Plant Nano Biology*, *10*, Article 100105. https://doi.org/10.1016/j.plana.2024.100105

Fusco, D., Colloca, G., Lo Monaco, M. R., & Cesari, M. (2007). Effects of antioxidant supplementation on the aging process. *Clinical Interventions in Aging*, *2*(3), 377–387.

Gao, H., Pang, Y., Li, L., Zhu, C., Ma, C., Gu, J., Wu, Y., & Chen, G. (2020). One-step synthesis of the nitrogen and sulfur codoped carbon dots for detection of lead and copper ions in aqueous solution. *Journal of Sensors*, *2020*(1), Article 8828456. https://doi.org/10.1155/2020/8828456

Gedda, G., Sankaranarayanan, S. A., Putta, C. L., Gudimella, K. K., Rengan, A. K., & Girma, W. M. (2023). Green synthesis of multi-functional carbon dots from medicinal plant leaves for antimicrobial, antioxidant, and bioimaging applications. *Scientific Reports*, *13*(1), Article 6371. https://doi.org/10.1038/s41598-023-33652-8

Gulcin, I. (2020). Antioxidants and antioxidant methods: An updated overview. *Archives of Toxicology*, *94*(3), 651–715. https://doi.org/10.1007/s00204-020-02689-3

Hasan, M. T., Gonzalez-Rodriguez, R., Ryan, C., Faerber, N., Coffer, J. L., & Naumov, A. V. (2018). Photo-and electroluminescence from nitrogen-doped and nitrogen–sulfur codoped graphene quantum dots. *Advanced Functional Materials*, *28*(42), Article 1804337. https://doi.org/10.1002/adfm.201804337

Hu, Q., Paau, M. C., Zhang, Y., Gong, X., Zhang, L., Lu, D., Liu, Y., Liu, Q., Yao, J., & Choi, M. M. F. (2014). Green synthesis of fluorescent nitrogen/sulfur-doped carbon dots and investigation of their properties by HPLC coupled with mass spectrometry. *RSC Advances*, *4*(35), 18065–18073. https://doi.org/10.1039/C4RA02170C

Huang, S.-W., Lin, Y.-F., Li, Y.-X., Hu, C.-C., & Chiu, T.-C. (2019). Synthesis of fluorescent carbon dots as selective and sensitive probes for cupric ions and cell imaging. *Molecules*, *24*(9), Article 1785. https://doi.org/10.3390/molecules24091785

Huang, Z., & Ren, L. (2025). Large scale synthesis of carbon dots and their applications: A review. *Molecules*, *30*(4), Article 774. https://doi.org/10.3390/molecules30040774

Ibrayev, N., Dzhanabekova, R., Seliverstova, E., & Amanzholova, G. (2022). Optical properties of N- and S-doped carbon dots based on citric acid and L-cysteine. *Fullerenes, Nanotubes and Carbon Nanostructures*, *30*(1), 22–26. https://doi.org/10.1080/1536383X.2021.1999933

Innocenzi, P., & Stagi, L. (2023). Carbon dots as oxidant-antioxidant nanomaterials, understanding the structure-properties relationship. A critical review. *Nano Today*, *50*, Article 101837. https://doi.org/10.1016/j.nantod.2023.101837

Ji, Z., Sheardy, A., Zeng, Z., Zhang, W., Chevva, H., Allado, K., Yin, Z., & Wei, J. (2019). Tuning the functional groups on carbon nanodots and antioxidant studies. *Molecules*, *24*(1), Article 152. https://doi.org/10.339/molecules24010152

Johny, A., da Silva, L. P., Pereira, C. M., & da Silva, J. C. G. E. (2024). Sustainability assessment of highly fluorescent carbon dots derived from eucalyptus leaves. *Environments*, *11*(1), Article 6. https://doi.org/10.3390/environments11010006

Kalogerakou, T., & Antoniadou, M. (2024). The role of dietary antioxidants, food supplements and functional foods for energy enhancement in healthcare professionals. *Antioxidants (Basel)*, *13*(12), Article 1508. https://doi.org/10.3390/antiox13121508

Karnwal, A., Jassim, A. Y., Mohammed, A. A., Sharma, V., Al-Tawaha, A. R. M. S., & Sivanesan, I. (2024). Nanotechnology for healthcare: Plant-derived nanoparticles in disease treatment and regenerative medicine. *Pharmaceuticals*, *17*(12), Article 1711. https://doi.org/10.3390/ph17121711

Kasif, M., Alarifi, A., Afzal, M., & Thirugnanasambandam, A. (2024). N, S-codoped carbon dots for antioxidants and their nanovehicle potential as molecular cargoes. *RSC Advances*, *14*(44), 32041–32052. https://doi.org/10.1039/d4ra05994h

Kumar, A., Kuang, Y., Liang, Z., & Sun, X. (2020). Microwave chemistry, recent advancements, and eco-friendly microwave-assisted synthesis of nanoarchitectures and their applications: A review. *Materials Today Nano*, *11*, Article 100076. https://doi.org/10.1016/j.mtnano.2020.100076

Li, L., Yu, B., & You, T. (2015). Nitrogen and sulfur co-doped carbon dots for highly selective and sensitive detection of Hg (II) ions. *Biosensors and Bioelectronics*, *74*, 263–269. https://doi.org/10.1016/j.bios.2015.06.050

Lin, H., Huang, J., & Ding, L. (2019). Preparation of carbon dots with high-fluorescence quantum yield and their application in dopamine fluorescence probe and cellular imaging. *Journal of Nanomaterials*, *2019*(1), Article 5037243. https://doi.org/10.1155/2019/5037243

Liu, J., Li, R., & Yang, B. (2020). Carbon dots: A new type of carbon-based nanomaterial with wide applications. *ACS Central Science*, *6*(12), 2179–2195. https://doi.org/10.1021/acscentsci.0c01306

Liu, M. (2020). Optical properties of carbon dots: A review. *Nanoarchitectonics*, *1*(1), 1–12. https://doi.org/10.37256/nat.112020124.1-12

Lobo, V., Patil, A., Phatak, A., & Chandra, N. (2010). Free radicals, antioxidants and functional foods: Impact on human health. *Pharmacognosy Reviews*, *4*(8), 118–126. https://doi.org/10.4103/0973-7847.70902

Lozano Pérez, A. S., Lozada Castro, J. J., & Guerrero Fajardo, C. A. (2024). Application of microwave energy to biomass: A comprehensive review of microwave-assisted technologies, optimization parameters, and the strengths and weaknesses. *Journal of Manufacturing and Materials Processing*, *8*(3), Article 121. https://doi.org/10.3390/jmmp8030121

Lu, H., Li, C., Wang, H., Wang, X., & Xu, S. (2019). Biomass-derived sulfur, nitrogen co-doped carbon dots for colorimetric and fluorescent dual mode detection of silver (I) and cell imaging. *ACS Omega*, *4*(25), 21500–21508. https://doi.org/10.1021/acsomega.9b03198

Magesh, V., Sundramoorthy, A. K., & Ganapathy, D. (2022). Recent advances on synthesis and potential applications of carbon quantum dots. *Frontiers in Materials*, *9*, Article 906838. https://doi.org/10.3389/fmats.2022.906838

Martemucci, G., Costagliola, C., Mariano, M., D'andrea, L., Napolitano, P., & D'Alessandro, A. G. (2022). Free radical properties, source and targets, antioxidant consumption and health. *Oxygen*, *2*(2), 48–78. https://doi.org/10.3390/oxygen2020006

Moammeri, A., Chegeni, M. M., Sahrayi, H., Ghafelehbashi, R., Memarzadeh, F., Mansouri, A., Akbarzadeh, I., Abtahi, M. S., Hejabi, F., & Ren, Q. (2023). Current advances in niosomes applications for drug delivery and cancer treatment. *Materials Today Bio*, *23*, Article 100837. https://doi.org/10.1016/j.mtbio.2023.100837

Molole, G. J., Gure, A., & Abdissa, N. (2022). Determination of total phenolic content and antioxidant activity of *Commiphora mollis* (Oliv.) Engl. resin. *BMC Chemistry*, *16*(1), Article 48. https://doi.org/10.1186/s13065-022-00841-x

Ngoc, L. T. N., Moon, J.-Y., & Lee, Y.-C. (2023). Plant extract-derived carbon dots as cosmetic ingredients. *Nanomaterials*, *13*(19), Article 2654. https://doi.org/10.3390/nano13192654

Ozyurt, D., Kobaisi, M. A., Hocking, R. K., & Fox, B. (2023). Properties, synthesis, and applications of carbon dots: A review. *Carbon Trends*, *12*, Article 100276. https://doi.org/10.1016/j.cartre.2023.100276

Pal, A., Sk, M. P., & Chattopadhyay, A. (2020). Recent advances in crystalline carbon dots for superior application potential. *Materials Advances*, *1*(4), 525–553. https://doi.org/10.1039/d0ma00108b

Qureshi, Z. A., Dabash, H., Ponnamma, D., & Abbas, M. K. G. (2024). Carbon dots as versatile nanomaterials in sensing and imaging: Efficiency and beyond. *Heliyon*, *10*(11), Article e31634. https://doi.org/10.1016/j.heliyon.2024.e31634

Ren, J., Malfatti, L., & Innocenzi, P. (2021). Citric acid derived carbon dots, the challenge of understanding the synthesis-structure relationship. *Journal of Carbon Research*, *7*(1), Article 2. https://doi.org/10.3390/c7010002

Romero, M. P., Alves, F., Stringasci, M. D., Buzza, H. H., Ciol, H., Inada, N. M., & Bagnato, V. S. (2021). One-pot microwave-assisted synthesis of carbon dots and *in vivo* and *in vitro* antimicrobial photodynamic applications. *Frontiers in Microbiology*, *12*, Article 662149. https://doi.org/10.3389/fmicb.2021.662149

Sadowska-Bartosz, I., & Bartosz, G. (2014). Effect of antioxidants supplementation on aging and longevity. *BioMed Research International*, *2014*(1), Article 404680. https://doi.org/10.1155/2014/404680

Samrot, A. V., Ram Singh, S. P., Deenadhayalan, R., Rajesh, V. V., Padmanaban, S., & Radhakrishnan, K. (2022). Nanoparticles, a double-edged sword with oxidant as

well as antioxidant properties—A review. *Oxygen*, *2*(4), 591–604. https://doi.org/10.3390/oxygen2040039

Sandhir, R., Yadav, A., Sunkaria, A., & Singhal, N. (2015). Nano-antioxidants: An emerging strategy for intervention against neurodegenerative conditions. *Neurochemistry International*, *89*, 209–226. https://doi.org/10.1016/j.neuint.2015.08.011

Shahid, K., Alshareef, M., Ali, M., Yousaf, M. I., Alsowayigh, M. M., & Khan, I. A. (2023). Direct growth of nitrogen-doped carbon quantum dots on Co_9S_8 passivated on cotton fabric as an efficient photoelectrode for water treatment. *ACS Omega*, *8*(44), 41064–41076. https://doi.org/10.1021/acsomega.3c03407

Sharma, N., Sharma, I., & Bera, M. K. (2022). Microwave-assisted green synthesis of carbon quantum dots derived from *Calotropis gigantea* as a fluorescent probe for bioimaging. *Journal of Fluorescence*, *32*(3), 1039–1049. https://doi.org/10.1007/s10895-022-02923-4

Suner, S. S., Sahiner, M., Ayyala, R. S., Bhethanabotla, V. R., & Sahiner, N. (2021). Versatile fluorescent carbon dots from citric acid and cysteine with antimicrobial, anti-biofilm, antioxidant, and AChE enzyme inhibition capabilities. *Journal of Fluorescence*, *31*(6), 1705–1717. https://doi.org/10.1007/s10895-021-02798-x

Swain, S., & Jena, A. K. (2025). Green synthesis of N,S-doped carbon dots from the giloy stem for fluorimetry detection of 4-nitrophenol, triple-mode detection of congo red, and antioxidant applications. *ACS Omega*, *10*(6), 5874–5885. https://doi.org/10.1021/acsomega.4c09748

Thanayutsiri, T., Patrojanasophon, P., Opanasopit, P., Ngawhirunpat, T., Plianwong, S., & Rojanarata, T. (2020). Rapid synthesis of chitosan-capped gold nanoparticles for analytical application and facile recovery of gold from laboratory waste. *Carbohydrate Polymers*, *250*, Article 116983. https://doi.org/10.1016/j.carbpol.2020.116983

Tian, X., Zeng, A., Liu, Z., Zheng, C., Wei, Y., Yang, P., Zhang, M., Yang, F., & Xie, F. (2020). Carbon quantum dots: In vitro and in vivo studies on biocompatibility and biointeractions for optical imaging. *International Journal of Nanomedicine*, *15*, 6519–6529. https://doi.org/10.2147/IJN.S257645

Tumilaar, S. G., Hardianto, A., Dohi, H., & Kurnia, D. (2024). A comprehensive review of free radicals, oxidative stress, and antioxidants: Overview, clinical applications, global perspectives, future directions, and mechanisms of antioxidant activity of flavonoid compounds. *Journal of Chemistry*, *2024*(1), Article 5594386. https://doi.org/10.1155/2024/5594386

Tungare, K., Bhori, M., Racherla, K. S., & Sawant, S. (2020). Synthesis, characterization and biocompatibility studies of carbon quantum dots from *Phoenix dactylifera*. *3 Biotech*, *10*(12), Article 540. https://doi.org/10.1007/s13205-020-02518-5

Umar, S., Farnandi, R., Salsabila, H., & Zaini, E. (2022). Multicomponent crystal of trimethoprim and citric acid: Solid state characterization and dissolution rate studies. *Open Access Macedonian Journal of Medical Sciences*, *10*(A), 141–145. https://doi.org/10.3889/oamjms.2022.7920

Wang, C.-Y., Ndaha, N., Wu, R.-S., Liu, H.-Y., Lin, S.-W., Yang, K.-M., & Lin, H.-Y. (2023). An overview of the potential of food-based carbon dots for biomedical applications. *International Journal of Molecular Sciences*, *24*(23), Article 16579. https://doi.org/10.3390/ijms242316579

Wang, D., Yan, Z., Ren, L., Jiang, Y., Zhou, K., Li, X., Cui, F., Li, T., & Li, J. (205). Carbon dots as new antioxidants: Synthesis, activity, mechanism and application in the food industry. *Food Chemistry*, *475*, Article 143377. https://doi.org/10.1016/j.foodchem.2025.143377

Waseem Basha, Z., Muniraj, S., & Senthil Kumar, A. (2024). Neem biomass derived carbon quantum dots synthesized via one step ultrasonification method for ecofriendly methylene blue dye removal. *Scientific Reports*, *14*(1), Article 9706. https://doi.org/10.1038/s41598-024-59483-9

Yalshetti, S., Thokchom, B., Bhavi, S. M., Singh, S. R., Patil, S. R., Harini, B. P., Sillanpää, M., Manjunatha, J. G., Srinath, B. S., & Yarajarla, R. B. (2024). Microwave-assisted synthesis, characterization and in vitro biomedical applications of *Hibiscus rosa-sinensis* Linn.-mediated carbon quantum dots. *Scientific Reports*, *14*(1), Article 9915. https://doi.org/10.1038/s41598-024-60726-y

Zehiroglu, C., & Ozturk Sarikaya, S. B. (2019). The importance of antioxidants and place in today's scientific and technological studies. *Journal of Food Science and Technology*, *56*(11), 4757–4774. https://doi.org/10.1007/s13197-019-03952-x

Zhang, T., Ji, Q., Song, J., Li, H., Wang, X., Shi, H., Niu, M., Chu, T., Zhang, F., & Guo, Y. (2022). Preparation of nitrogen and sulfur co-doped fluorescent carbon dots from cellulose nanocrystals as a sensor for the detection of rutin. *Molecules*, *27*(22). Article 8021. https://doi.org/10.3390/molecules27228021

Zhang, W., Chavez, J., Zeng, Z., Bloom, B., Sheardy, A., Ji, Z., Yin, Z., Waldeck, D. H., Jia, Z., & Wei, J. (2018). Antioxidant capacity of nitrogen and sulfur codoped carbon nanodots. *ACS Applied Nano Materials*, *1*(6), 2699–2708. https://doi.org/10.1021/acsanm.8b00404

Zhang, Y., & He, J. (2015). Facile synthesis of S, N co-doped carbon dots and investigation of their photoluminescence properties. *Physical Chemistry Chemical Physics*, *17*(31), 20154–20159. https://doi.org/10.1039/c5cp03498a

Zhou, H., Ren, Y., Li, Z., He, W., & Li, Z. (2022). Selective detection of Fe^{3+} by nitrogen–sulfur-doped carbon dots using thiourea and citric acid. *Coatings*, *12*(8), Article 1042. https://doi.org/10.3390/coatings12081042